Monthly Notices of the ROYAL ASTRONOMICAL SOCIETY

MNRAS **499,** 106–115 (2020) doi:10.1093/mnras/staa2820
Advance Access publication 2020 September 18

Constraining protoplanetary discs with exoplanetary dynamics: Kepler-419 as an example

Mohamad Ali-Dib[1,2]★ and Cristobal Petrovich[3,4]

[1]*Institut de recherche sur les exoplanètes, Université de Montréal, 2900 boul. Édouard-Montpetit, Montréal H3T 1J4, Canada*
[2]*Centre for Planetary Sciences, University of Toronto Scarborough, Toronto, Ontario M1C 1A4, Canada*
[3]*Steward Observatory, University of Arizona, 933 N. Cherry Ave., Tucson, AZ 85721, USA*
[4]*Canadian Institute for Theoretical Astrophysics, 60 St. George St., Toronto, ON M5S 3H8, Canada*

Accepted 2020 September 12. Received 2020 September 9; in original form 2020 July 14

ABSTRACT

We investigate the origins of Kepler-419, a peculiar system hosting two nearly coplanar and highly eccentric gas giants with apsidal orientations liberating around anti-alignment, and use this system to place constraints on the properties of their birth protoplanetary disc. We follow the proposal by Petrovich, Wu, & Ali-Dib that these planets have been placed on these orbits as a natural result of the precessional effects of a dissipating massive disc and extend it by using direct *N*-body simulations and models for the evolution of the gas discs, including photoevaporation. Based on a parameter space exploration, we find that in order to reproduce the system the initial disc mass had to be at least 95 $M_{\rm Jup}$ and dissipate on a time-scale of at least 10^4 yr. This mass is consistent with the upper end of the observed disc masses distribution, and the dissipation time-scale is consistent with photoevaporation models. We study the properties of such discs using simplified 1D thin-disc models and show that they are gravitationally stable, indicating that the two planets must have formed via core accretion and thus prone to disc migration. We hence finally investigate the sensitivity of this mechanism to the outer planet's semimajor axis, and find that the nearby 7:1, 8:1, and 9:1 mean-motion resonances can completely quench this mechanism, while even higher order resonances can also significantly affect the system. Assuming the two planets avoid these high-order resonances and close encounters, the dynamics seems to be rather insensitive to planet c semimajor axis, and thus orbital migration driven by the disc.

Key words: planets and satellites: formation – planet–disc interactions.

1 INTRODUCTION

Kepler-419 is a two gas giants system with well-characterized architecture. The two planets *b* and *c* are respectively 2.77 and 7.65 Jupiter masses, orbiting at 0.374 and 1.697 au, with eccentricities of 0.81 and 0.18, in apsidally anti-aligned orbits ($\varpi_{\rm b} - \varpi_{\rm c} \sim 180$ deg) (Ford et al. 2012; Dawson et al. 2014; Almenara et al. 2018). The origins of these unique orbits merit an explanation. Petrovich, Wu & Ali-Dib (2019) (PWA19) showed using secular theory (approximate orbit-averaged equations of motion) that the system could have originated in the inner gap of a slowly dissipating massive disc that forced the apses to anti-align through its precessional effects. The general dynamics and eccentricity evolution of exoplanets due to disc dispersal were initially explored by Nagasawa, Lin & Ida (2003). In this mechanism, the system needs to start with an angular momentum deficit (AMD) for planet *c*, that is transferred in the process to planet b. PWA19 proposed that this initial AMD might be due to either planet–disc interactions where the outer Lindblad resonances can increase the planet's eccentricity (Bitsch et al. 2013), or from planet–planet scattering (Lega, Morbidelli & Nesvorný 2013). It is unlikely however that scattering alone can lead to an anti-aligned and nearly coplanar system (Barnes & Greenberg 2006; Chatterjee et al. 2008), hence the need for the disc dispersal mechanism. We refer the reader to PWA19 for further background discussions.

An alternative explanation was proposed by Jackson, Dawson & Zalesky (2019), who showed using *N*-body integrations that for a small region of parameter space, the presence of an undetected third planet could excite planet b's eccentricity periodically without distabilizing the system. In this paper, we build on and extend the work of PWA19. We first verify the accuracy of their results using *N*-body integrations and do a parameter study over disc mass and dispersal time-scale to constrain the values allowing the formation of Kepler-419 (Sections 3 and 4). We then study the properties of these discs and compare them against observations to verify the realism of this idea (Section 4.2). We finally study the effects of changing planet c's semimajor axis to understand the sensitivity of the system (and formation mechanism) to this parameter (Section 4.3).

2 NUMERICAL SET-UP

All simulations in the work were done using the `REBOUND` *N*-body integrator (Rein & Liu 2012; Rein & Spiegel 2015; Rein & Tamayo 2015), along with its `REBOUNDx` add-ons package (Tamayo et al. 2020). Simulations were mostly done using the symplectic Wisdom–Holman integrator `WHFAST`, unless otherwise is explicitly stated. This is because we are only interested in the evolution of stable systems that do not undergo close encounters. The system

★ E-mail: m.alidib@utoronto.ca

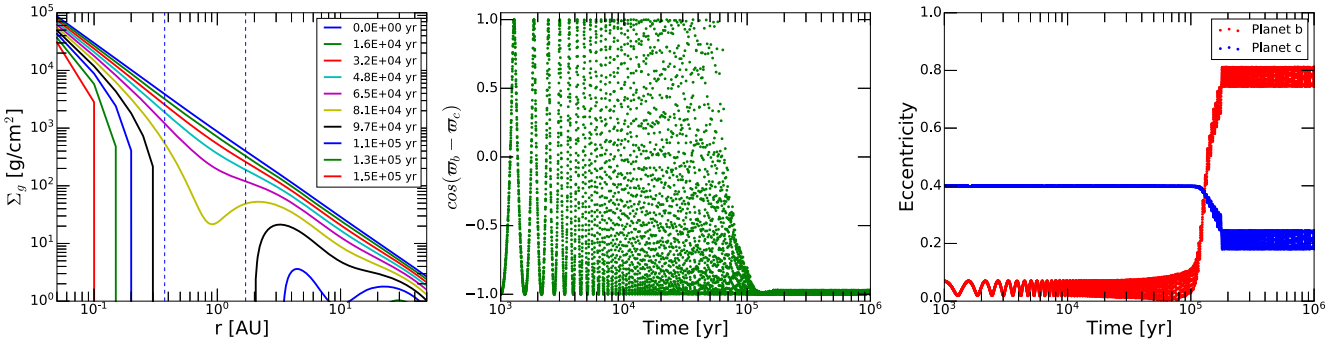

Figure 1. The evolution of a two planets system into Kepler-419 in a photoevaporating disc. Left: Time evolution of the gas surface density profile of a disc governed by equation (2). Centre: The apses of the two planets are forced into anti-alignment by the disc's precession, and then remain in this state due to its adiabatic dispersal. Right: Starting with an AMD, the eccentricity of planet b increases from a near zero to ∼0.8, while that of planet c decreases from the initial 0.4 to ∼0.2.

is integrated with a time-step equal to 0.025× the smallest orbital period in the system. All simulations are run for 6×10^6 yr. The disc potential is implemented following Binney & Tremaine (2008) eq. 2.156, leading to the radial acceleration:

$$\frac{F_{\rm D}(r)}{m} = \frac{4G}{r}\int_0^r {\rm d}a \frac{a}{\sqrt{r^2-a^2}}\frac{\rm d}{{\rm d}a}\int_a^\infty {\rm d}r' \frac{r'\Sigma\left(r'\right)}{\sqrt{r'^2-a^2}}, \quad (1)$$

where we are setting to 0 the z component of the potential, and hence are not considering its effects on the inclinations of the system. In fact we treat the system purely as two-dimensional, in contrast with the 3D treatment of PWA19.

The disc force is implemented using the `add_custom_force` method of `REBOUNDx`.

For all cases, we initiate the system with a 1.39 $M_\odot$ star, and two planets b and c of 2.77 and 7.65 $M_{\rm J}$. Their respective initial eccentricities are set to 0.05 and 0.4 (following PWA19), while inclinations and longitudes of ascending nodes are set to 0. We again follow PWA19 by initially setting $\omega_{\rm b} - \omega_{\rm c} = 60^\circ$.

3 KEPLER-419: PLANETS FULLY EMBEDDED IN A PHOTOEVAPORATING DISC

For the system's secular dynamics to evolve as suggested by Petrovich et al. (2019), a main requirement is for the two planets to be located inside a common gap, with a massive disc beyond their orbits. One possible physical mechanism for this scenario is a photoevaporating disc, where the planets are initially fully embedded in a disc with no cavity, then photoevaporation slowly carves up a gap in the inner disc.

Here, we test this hypothesis numerically using our set-up, and assuming a disc surface density profile that evolves as a function of time as

$$\Sigma(r,t) = \Sigma_0(r) - \dot{\Sigma}_w \times \Delta t, \quad (2)$$

where $\Sigma_0(r)$ is defined through the following functional form:

$$\Sigma(R) = \Sigma_0 \left(\frac{r}{r_{\rm in}}\right)^{-\gamma}, \quad (3)$$

where Σ_0 is one of the main parameters we vary, $r_{\rm in}$ is set to 0.05 au, and γ is fixed at 1.5. The outer edge of the disc is always kept at 50 au. The photoevaporation rate $\dot{\Sigma}_w$ is defined following the functional fit to hydrodynamic simulations of Owen, Clarke & Ercolano (2012):

$$\dot{\Sigma}_w(y) = \left[\frac{a_2 b_2 \exp\left(b_2 y\right)}{R} + \frac{c_2 d_2 \exp\left(d_2 y\right)}{R} + \frac{e_2 f_2 \exp\left(f_2 y\right)}{R}\right] \times \exp\left[-\left(\frac{y}{57}\right)^{10}\right] \quad (4)$$

and $\dot{\Sigma}_w(y<0) = 0$, where

$$y = 0.95\frac{(R - R_{\rm hole})}{1\ {\rm au}}\left(\frac{M_*}{1\ {\rm M}_\odot}\right)^{-1} \quad (5)$$

and the dimensionless constants are $a_2 = -0.438\,226$, $b_2 = -0.106\,583\,87$, $c_2 = 0.569\,9464$, $d_2 = 0.010\,732\,277$, $e_2 = -0.131\,809\,597$, $f_2 = -1.322\,857\,09$.

We use $R_{\rm hole} = 0.05$ au. We normalize this photoevaporation rate by 10^8, to get a total mass loss of $6 \times 10^{-8}\ {\rm M}_\odot\ {\rm yr}^{-1}$.

The system's evolution is shown in Fig. 1. The disc starts with a mass of ∼10 $M_{\rm J}$. Photoevaporation then disperses the disc on a time-scale of $\sim 10^5$ yr, opening a gap spanning the region between the two planets after $\sim 8 \times 10^4$ yr. At this point ∼5 $M_{\rm J}$ of gas is remaining outside the orbit of planet c. Before the gap opening, planet c eccentricity remains constant while planet b's oscillate with moderate amplitude, consistent with the Laplace–Lagrange solution for two planets orbiting a star, with the axi-symmetric disc having no effect as the two planets are still fully embedded. When the gap is opened at $\sim t = 8 \times 10^4$ yr however, angular momentum exchange proceeds with planet b's eccentricity increasing quickly to 0.8, and planet c's decreasing to 0.2, values consistent with current observations of Kepler-419. Finally, the gap opening is followed by the anti-alignment of the planets apses, the second major dynamical characteristic of Kepler-419.

In reality however, this approach is not truly self-consistent since, as shown in Section 4.2, planets this massive will open deep gaps in the disc that are wide enough to merge, quickly clearing up the disc regions interior to the outer planet. In Section 4, we consider a more realistic, although simpler, set-up where the planets start embedded in a common gap. The dynamics considered in the current section however might still be relevant for sub-Neptunes not capable of fully carving gaps. For more sophisticated models of disc evolution with planet-carved gaps, we refer the reader to the recent work by Toliou, Tsiganis & Tsirvoulis (2019).

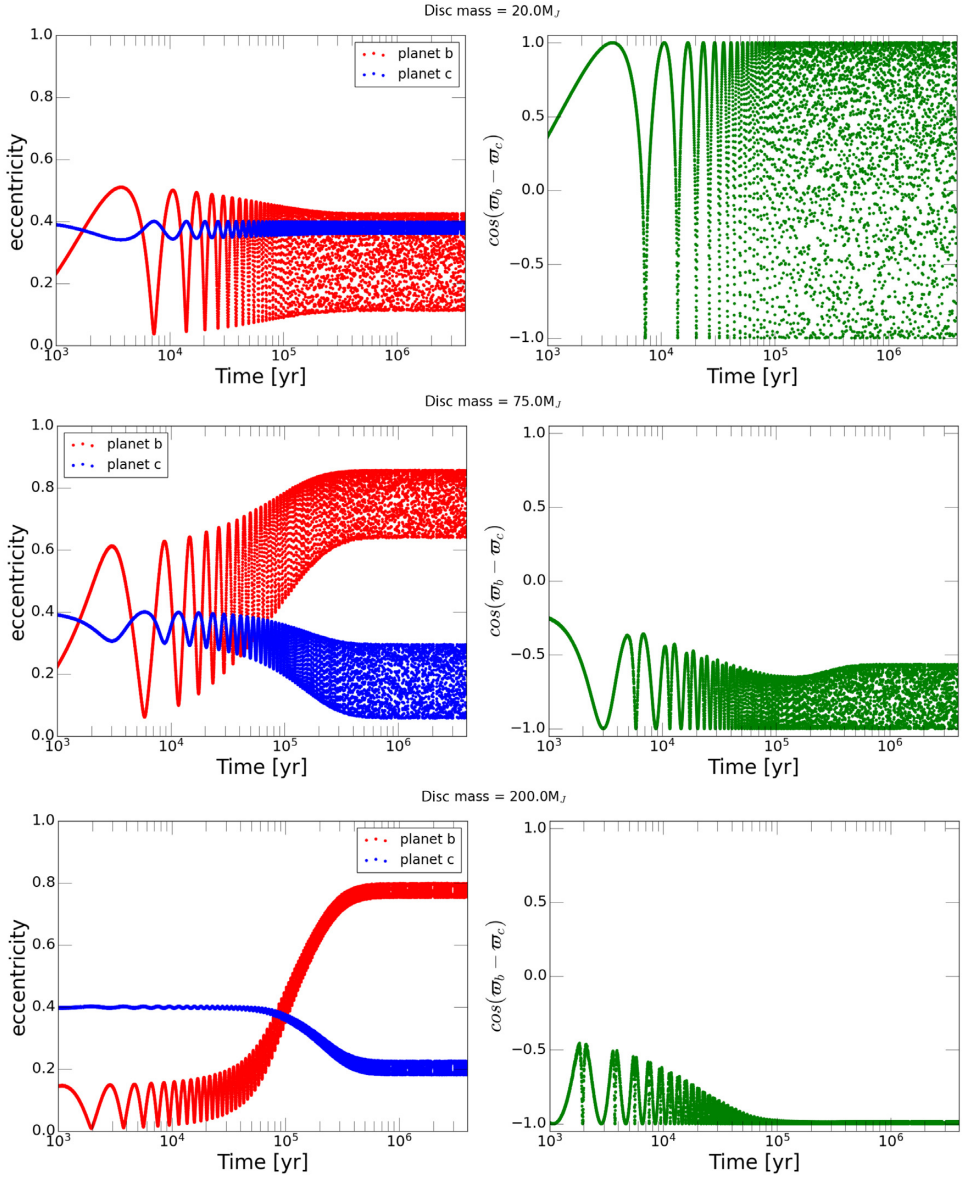

Figure 2. Examples for typical behaviours observed in our Kepler-419 like set-ups, for three disc mass values, and $\tau_d = 10^5$ yr. Top: The disc mass is too low to have any effects on the system evolution. Middle: Transition case where the disc mass forces the planets apses into anti-alignment but with noticeable oscillation amplitudes. Bottom: Massive disc leading to Kepler-419 like system with low oscillation amplitudes.

4 KEPLER-419: PARAMETERS STUDY

In this section, we investigate the disc mass and dispersal time-scales needed for a two-planet system to evolve into Kepler-419 like configuration. We hence generate and evolve a large number of systems while varying two parameters: (1) the disc mass through Σ_0 in equation (3), and (2) the disc's dispersal time-scale τ_d. Therefore, instead of using equation (2) as above, we simply the scheme by assuming the disc mass to decrease as $M^{t0}_{disc} \exp(-t/\tau_d)$. This implies that the disc is dissipating simultaneously at all radii, rather than inside-out as suggested by photoevaporation models.

This is however justifiable, since, within the simplifications of the model (axisymmetric disc, no feedback from the planet on to the disc), the dynamics we are interested in has a stronger dependence on the disc's total mass, than on its distribution. This is shown in PWA19's equations 9 and 11 where for a minimal mass solar nebula density profile: $\dot{\varpi}_p \propto M_{disc}/\sqrt{r_{out}}$ for a given r_{in}.

We set r_{in} in equation (3) to $1.5\times$ a_c au with $\Sigma(r < r_{in}) = 0$ to emulate a gap, and the semimajor axis of planets b and c to respectively 0.374 and 1.697.

We try disc masses of 1, 20, 40, 50, 75, 100, and 200 M_{Jup}. The higher values are probably unrealistic as such massive discs can be prone to gravitational instabilities, but we include them as limiting cases. We explore disc dispersal time-scales τ_d of 10^4, 10^5, and 10^6 yr.

4.1 Disc mass and dispersal time-scale

In Fig. 2, we show the time evolution of the planets' eccentricities and apses for three representative cases, with the full results for all cases shown in appendix Figs A1 and A2.

In this plot, we identify multiples distinct regimes. For $M_d = 1$ and $20\,M_{Jup}$, the disc mass is small enough for the disc-planet potential to be weak compared to that planet–planet interaction

potential. Hence, this case is equivalent to a three-body problem with a central star and two significantly less massive planets where the eccentricities are secularly forced and the apses circulate. This problem is well described by the classical Laplace–Lagrange secular theory (Murray & Dermott 2000).

On the other extreme end, for the massive discs with $M_{\rm d} \geq 75\,M_{\rm Jup}$, we recover the results of PWA19 remarkably. In all of these cases, the apsidal precession of the planets is dominated by the disc, rather than the planet–planet secular interactions. The apses therefore always evolve into liberating around anti-alignment, while the AMD is transferred from planet c to planet b, giving eccentricities consistent with Kepler-419 as seen again in Fig. 2. Finally, for the intermediate cases of $M_{\rm d} \sim 40$–$50\,M_{\rm Jup}$, we do see possible evolution towards (sometimes transient) anti-aligned apses, however the amplitude of the oscillations are very large and thus we consider this case incompatible with Kepler-419. The same can be said for the eccentricities.

We identify the minimal disc mass necessary for a Kepler-419 like system to be around 75 $M_{\rm J}$, a value few times higher than that used in Section 3 where the system did evolve into K419. The two set-ups however are not fully equivalent. In Section 3, the planets start fully embedded in the disc, and hence the precession rate of the planets is retrograde (e.g. Rafikov & Silsbee 2015) and dominated by the inner planet ($|\dot{\varpi}_{\rm in}| \propto M_{\rm disc} n_{\rm in}$). In both cases, we have $\Delta\dot{\varpi} \equiv \dot{\varpi}_{\rm out} - \dot{\varpi}_{\rm in} > 0$ initially, allowing the resonance to be crossed ($\Delta\dot{\varpi} = 0$) in a similar fashion. However, the mass of the disc required to cross the resonance is lower in the embedded case roughly by a factor of $n_{\rm in}/n_{\rm out} = P_{\rm out}/P_{\rm in} \sim 9$, which is roughly consistent with the ratio of the minimal disc masses ($\sim 75\,M_{\rm J}/10\,M_{\rm J} = 7.5$) between the fully embedded simulations and this case.

It is interesting that Kepler-419 is recovered even for discs dispersing on a 10^4 yr time-scale, an order of magnitude lower than the value assumed by PWA19. This is reassuring since in photoevaporation models, once an inner cavity has been carved (which is our starting assumption), discs usually proceed to disperse inside-out very quickly due to direct stellar irradiation. This puts a constraint on the amount of 'adiabacity' necessary for this mechanism to operate. Notice that, as one would expect, for a fixed disc mass, longer disc dispersal time-scales lead to the same end results, but over longer time. On the other hand for fixed $\tau_{\rm d}$ but increasing the disc mass, the amplitude of the secular oscillations around the equilibrium values of the eccentricity and apses decreases.

4.2 Properties of the natal disc

In this section, we analyse the properties of our lowest mass disc compatible with Kepler-419, that is 75 $M_{\rm J}$ ($\sim$0.075 $M_\odot$). First, we compare this disc to observations. In a recent ALMA survey of the Lupus complex, Ansdell et al. (2016) found dust masses ranging from $\sim$0.3 to 100 $M_\oplus$, while their gas masses where mostly below Jupiter mass, and almost all of them below the MMSN (10^{-2} $M_\odot$, 10 $M_{\rm J}$). Pascucci et al. (2016) and Long et al. (2017) also used ALMA to measure the dust mass in the Chamaeleon I star-forming region, and found a mass range consistent with Ansdell et al. (2016). Gas masses as measured in the infrared (with HD lines) seem to be higher, where McClure et al. (2016) for example constrained the masses of GM Aur and DM Tau to respectively 2.5–20.4 $\times\ 10^{-2}$ and 1.0–4.7 $\times\ 10^{-2}$ $M_\odot$. Bergin et al. (2013) on the other hand found a lower mass limit of TW Hya around 0.05 $M_\odot$ (50 $M_{\rm J}$). Our lowest mass disc hence lies towards the upper end of these distributions. Note that estimating disc gas mass from CO lines is problematic, as it depends on the assumed CO/H_2 ratio, that is affected by the complex physical chemistry of CO. Yu et al. (2017) for example found that CO observations underestimate gas mass by an order of magnitude. The values reported above are hence probably lower limits in most cases. Note that since dust mass is measured using the sub-millimetre continuum flux that is insensitive to solids larger than $\sim$cm, dust masses are also lower limits that does not account for the total solids budget. Dust mass is hence a bad tracer for the total disc's mass, even when the stellar metallicity is known.

To fully understand the Kepler-419 birth protoplanetary disc, we need to account for the planets mass as well. This increases our minimal mass disc to 95.07 $M_{\rm J}$ (0.094 $M_\odot$), still around the uppermost limits of the observed population. Assuming ISM dust/gas ratio of 0.01, the minimal mass dust disc is $\sim$300 $M_\oplus$, a factor of few times above the upper limits of the measured values. On the M_*–$M_{\rm dust}$ diagrams of Ansdell et al. (2017), our minimal mass disc fit on the curves found for the younger discs in Taurus, Lupus, and Cham I.

Our minimal mass K419 disc can moreover be compared to transitional discs with a large inner cavity. These discs are an intermediate step between photoevaporating protoplanetary discs and debris discs. A *Spitzer* survey of $\sim$150 transition discs by van der Marel et al. (2016) found that $\sim$7 per cent of their sample has a total mass $\geq$100 $M_{\rm J}$, even though there is a much higher fraction with masses between 10 and 100 $M_{\rm J}$. These masses were obtained through (dust) SED fitting by `RADMC-3D` radiative transfer models, assuming ISM dust to gas ratio and account for dust growth using the prescription of Andrews et al. (2011). A *Herschel* data analysis of Chamaeleon I by Ribas et al. (2016) found that SZ Cha and CS Cha have respectively $M_{\rm dust} = 10^{-3.4}$ and $10^{-3.8}$ $M_\odot$, implying roughly $10^{-1.6}$ $M_\odot$ total mass. This is a factor of 3 times less than our minimal disc. Finally, a recent complete ALMA survey of the Lupus star-forming region by van der Marel et al. (2018) found that 3 out of 11 discs have dust masses consistent with our minimal mass disc. Therefore, transition discs massive enough to form K419 are consistent with observations. Note that, strictly speaking, transition discs masses should be compared only to the minimum disc mass excluding the actual planets (75 $M_{\rm J}$), while protoplanetary disc masses should be compared to the minimal disc in addition to the planets (95 $M_{\rm J}$). The significant uncertainties on the disc masses, due to both observational error bars and the modelling assumptions, render this distinguishment unnecessary however.

Now we focus on the possible formation pathways for the Kepler-419 planets. Since a very massive disc is needed to form the system, we investigate whether such a disc is gravitationally stable. We hence construct a standard radiative steady-state thin disc (Pringle 1981), as described in Ali-Dib, Cumming & Lin (2020). This gives

$$T_{\rm d,rad} = T_{\rm s}^{4/5} \left(\frac{\kappa \mu \Omega \dot{M}}{6\pi\alpha k_{\rm B}\gamma}\right)^{1/5} = 373\ {\rm K}\ r_{\rm au}^{-9/10}\alpha_{-2}^{-1/5}\dot{M}_{-7.5}^{2/5}\left(\frac{M_\star}{{\rm M}_\odot}\right)^{3/10}\left(\frac{\kappa}{{\rm cm^2\ g^{-1}}}\right)^{1/5}, \quad (6)$$

where $\alpha_{-2} = \alpha/0.01$ and $\dot{M}_{-7.5} = \dot{M}/10^{-7.5}$ $M_\odot$ yr^{-1}. The density is then

$$\rho_{d,\rm rad} = 1.7\times10^{-10}\ {\rm g\ cm^{-3}}\ r_{\rm au}^{-33/20}\alpha_{-2}^{-7/10}\dot{M}_{-7.5}^{2/5} \times\left(\frac{M_\star}{{\rm M}_\odot}\right)^{11/20}\left(\frac{\kappa}{{\rm cm^2\ g^{-1}}}\right)^{-3/10}. \quad (7)$$

We hence control three disc parameters: turbulence viscosity parameter α, the disc opacity κ, and its accretion rate on to the star $\dot{M}$. We try $\alpha = 10^{-2}$ and 10^{-4}, in addition to $\kappa = 1$ and 0.01. For each case, we change the $\dot{M}$ value to get the total disc mass we

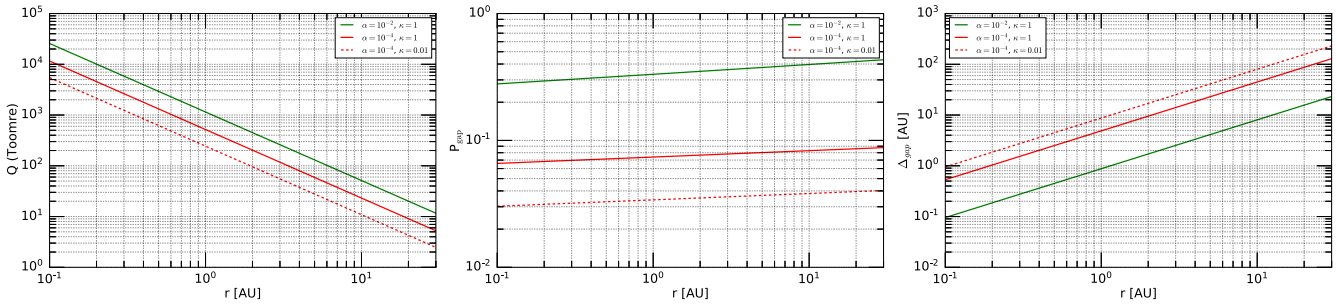

Figure 3. Left: The Toomre stability parameter Q for our minimal mass Kepler-419 disc, for different values of turbulent viscosities α and disc opacity κ. In all cases, the disc is fully stable against gravitational collapse in the entire planet formation region. Centre: The value of the gap opening criteria function $P_{\rm gap}$ as defined in equation (9), for a 2.77 $M_{\rm J}$ planet. $P_{\rm gap}$ is significantly lower than 1 throughout the disc, indicating that this planet is capable of carving a deep cavity anywhere. Right: The width of the gap opened by a 2.77 $M_{\rm J}$, as calculated through equation (10). For all parameters, a gap carved by a planet at 1.7 au is deep enough to reach the inner Kepler-419 planet no matter its mass, allowing the two planets to be embedded inside a common gap, without the need for photoevaporation.

need. We finally calculate the Toomre parameter:

$$Q \equiv \frac{c_{\rm s}\Omega}{\pi G \Sigma}, \tag{8}$$

where $Q < 1$ for gravitationally unstable discs. We plot Q in Fig. 3 (left-hand panel) for our three disc models: highly turbulent with high opacity ('hot' disc), and weakly turbulent with both high and low opacity.

We find that, in all cases, $Q \gg 1$ everywhere in the planet-forming regions of these discs inside 30 au These massive discs are hence gravitationally stable under our simplified assumptions. While it is conceivable that gravitational collapse can take place in the outermost parts of the disc (where it is usually thought to operate), a gas giant will only undergo the slow type II migration on a time-scale of r^2/ν. For $r = 30$ au and $\nu \sim 10^{15}$ cm^2 s^{-1}, $t_{\rm mig} \sim 6 \times 10^6$ yr, which is comparable to the disc lifetime. Assuming these calculations stands for more sophisticated disc and migration models with proper radiative transfer, this imply that the Kepler-419 planets probably formed via core accretion.

It is also of interest to check whether the Kepler-419 planets are capable of carving gaps in such massive discs. This is an important self-consistency check since an inner gap in the disc embedding both planets is a prerequisite for the secular dynamics we are considering, and this can be an alternative to the photoevaporation carved gap discussed in Section 3. Crida, Morbidelli & Masset (2006) showed that for a planet embedded in a disc to open a gap, the following condition needs to be satisfied:

$$P_{\rm gap} \equiv \frac{3}{4}\frac{H}{R_{\rm H}} + \frac{50}{q\mathcal{R}} \lesssim 1, \tag{9}$$

where $R_{\rm H}$ is the planet's Hill radius, $q = M_{\rm p}/M_{\rm s}$, and $\mathcal{R} = r_{\rm p}^2\Omega_{\rm p}/\nu$ is the Reynolds number. In Fig. 3 (centre), we plot this quantity for our disc models, and $M_{\rm p} = 2.77\ M_{\rm J}$. We find the condition to be satisfied throughout the disc for both $\alpha = 10^{-4}$ and 10^{-2}. This imply that the Kepler-419 planets can indeed open gaps in these massive discs.

We finally calculate the gaps' widths following Kanagawa et al. (2016):

$$\frac{\Delta_{\rm gap}}{R_{\rm p}} = 0.41 \left(\frac{M_{\rm p}}{M_*}\right)^{1/2} \left(\frac{h_{\rm p}}{R_{\rm p}}\right)^{-3/4} \alpha^{-1/4} \tag{10}$$

with the results shown in Fig. 3 (right). Even for $\alpha = 10^{-2}$, the gaps are found to be wide enough to merge, allowing the two planets to coexist inside one common gap. This implies that a photoevaporation driven inner disc gap is not the only possible formation channel for Kepler-419, as the planets are massive enough to exist within a common gap anyway.

4.3 Sensitivity of the results to $P_{\rm c}$

If the Kepler-419 planets formed via core accretion as argued above, then it is likely they underwent disc migration at some point in their history. This is especially true for massive discs, since the time-scale of type I migration is $\propto \Sigma_{\rm g}$. In this section, we hence explore the dependence of Kepler-419's architecture on the semimajor axis / period of planet c, that we now free as a parameter. In Fig. 4, we show the end results of simulations where we changed the period of planet c for values ranging between 6 and 13 $\times$ $P_{\rm b}$. The actual value for Kepler-419 is $P_{\rm c} = 9.6\ P_{\rm b}$. We use the same disc mass range (20–200 $M_{\rm J}$), and a fiducial dispersal time-scale of 10^5 yr.

Multiple distinct dynamical regimes can be identified in this plot.

Green circles in Fig. 4 represent systems that evolved into a Kepler-419 like architecture, with anti-aligned apses, and the observed eccentricities of both planets. These are mainly cases with $P_{\rm c} > 8\times\ P_{\rm b}$ and $M_{\rm d} \geq 50\ M_{\rm J}$. We moreover notice that the minimum disc mass needed for the system to follow this evolution channel decreases with $P_{\rm c}$: while 75 $M_{\rm J}$ are needed for the $P_{\rm c} = 9.6\ P_{\rm b}$, only 40 $M_{\rm J}$ are needed for $P_{\rm c} = 13\ P_{\rm b}$. This can be readily understood within the framework of PWA19's analytic model where planet c' precession time-scale due to the disc is $\propto P_{\rm c}/M_{\rm d}$.

Blue circles on the other hand are systems that are either completely stable (with no apsidal liberation or AMD exchange between the two planets), or with minor dynamical evolution that does not evolve the system into Kepler-419 (mostly moderate amplitude secular oscillations). This is the case for low disc masses that are unable to significantly affect the system's dynamics, reducing the set-up into a classic three-body problem with an inner test particle and external perturber. More interestingly, this is also the case for some of the MMR cases, even for high disc masses. Prominent examples are the 6:1, 7:1, and 8:1 resonance for almost all disc masses.

Pink circles are systems that undergo significant dynamical evolution without transforming into K419. This is an umbrella for a plethora of different behaviours. For $M_{\rm d} = 40\ M_{\rm J}$ for example, while planet b's eccentricity does increase significantly while that of planet c is decreasing, the amplitudes of the eccentricities secular oscillations is very large. Moreover, while the planets' apses do anti-align, this state in these cases is transient. An intriguing case is

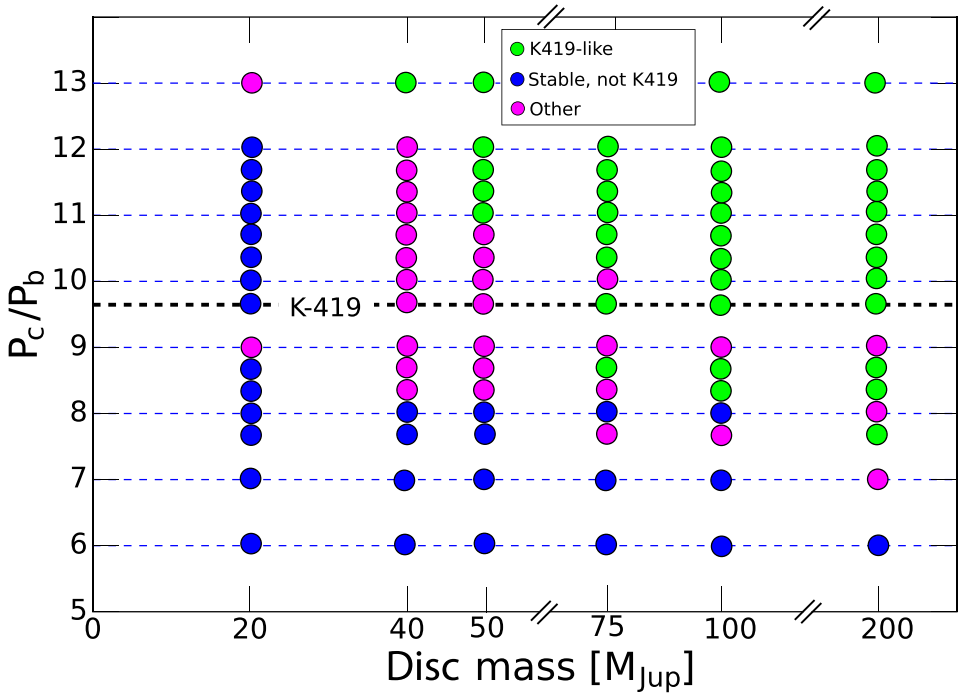

Figure 4. The effects of relatively small changes in the period (thus semimajor axis) of planet c. Blue circles are systems that become stable, with little to no eccentricity or apsidal evolutions, and low amplitude secular oscillations. Green circles represent cases that evolve into Kepler-419 like systems where the apses liberate around anti-alignment. Finally, pink circles on the other hand are systems that does not fit either of the previous two categories. Notice the multiple breaks in the *x*-axis scale.

that of the 9:1 MMR where no AMD exchange takes place between the planets at all, but their apses do liberate stably around anti-alignment. For periods slightly smaller or larger than this exact commensuration however, the system evolves cleanly into Kepler-419. The 10:1 MMR is also a unique case, where the planets' follow a dynamically very 'noisy' Kepler-419 like evolution, before exiting the anti-aligned mode. A third category included in the pink circles is for example the 7:1 and 8:1 MMR for $M_d = 200\ M_J$, where the system does evolve into K419-like state, but remains dynamically very noisy, even after the disc's dissipation. In this case, the disc contribution to the Hamiltonian is clearly of the same magnitude as the MMR.

The analytical Hamiltonian of PWA19 did not include any resonant terms, and these results indicates that even very high-order MMRs can play an important role in exoplanetary dynamics.

To check whether these variations are indeed caused by high-order MMRs, we plot in Fig. 5 the system short-term evolution in the pseudo coordinate-momentum pair ($e_b \cos[\varpi_b - \varpi_c]$, $e_b \sin[\varpi_b - \varpi_c]$) phase space for three cases: $P_c = 9.0$, 9.6, and 10.0 P_b. We notice the appearance of new high-frequency modes for the 9:1 and 10:1 MMR, and their complete absence outside of these resonances when $P_c = 9.6\ P_b$. The amplitude of these modes moreover seems to decrease with the increasing resonance order, implying furthermore that they are indeed MMRs related. Representative cases from this section were verified using the very high accuracy non-symplectic integrator `IAS15`.

In conclusion, for high enough disc masses, while there are large parts of P_c–M_d parameter space where the system can evolve into Kepler-419, other end results are also possible. Two planets should not get trapped in certain higher order MMRs, or be close enough to undergo close encounters. Kepler-419 like systems might hence be more common than currently thought, and future observations can confirm or rule this out. The detailed eccentricity and apses evolution of all of these cases in shown in the appendix in Figs A3 and A4.

5 DISCUSSIONS AND CONCLUSIONS

In this paper, we studied the origins of the highly eccentric, apsidally anti-aligned, two giant planets Kepler-419 system using *N*-body simulations where we introduced a dissipating protoplanetary disc's potential as an extra force. We first show that the analytical results of PWA19 are recovered accurately, indicating that secular theory is adequate to describe the system's evolution with no significant effects from the ignored parts of the Hamiltonian. By exploring a large range of disc masses, we show that the minimum disc mass to retrieve Kepler-419 is 75 Jupiter masses, increasing to 95 Jupiter masses if we are to include the planets themselves. These values are consistent with values found in the infrared with Herschel, and lie towards the upper range of masses measured with ALMA, but CO-based observations are probably underestimating the gas mass significantly. Furthermore, Kepler-419 is recovered even for dissipation time-scales as low as 10^4 yr, consistent with photoevaporation models. We then used a simple 1D α-disc model to study the stability of a protoplanetary disc this massive, and find the Toomre Q parameter to be significantly larger than unity for all reasonable radii. This implies that the Kepler-419 planets, massive as they are, probably formed via core accretion.

Finally, we ran simulations while varying the period of planet *c*, and find that higher order MMRs such as the 8:1, 9:1, and 10:1 can either completely stabilize the system against the disc's precessional effects, or sometimes render its evolution dynamically noisy.

Our results indicate that K419-like systems with highly eccentric apsidally anti-aligned planets might not be uncommon. Considering the set of all confirmed planets in the `exoplanets.eu` catalogue

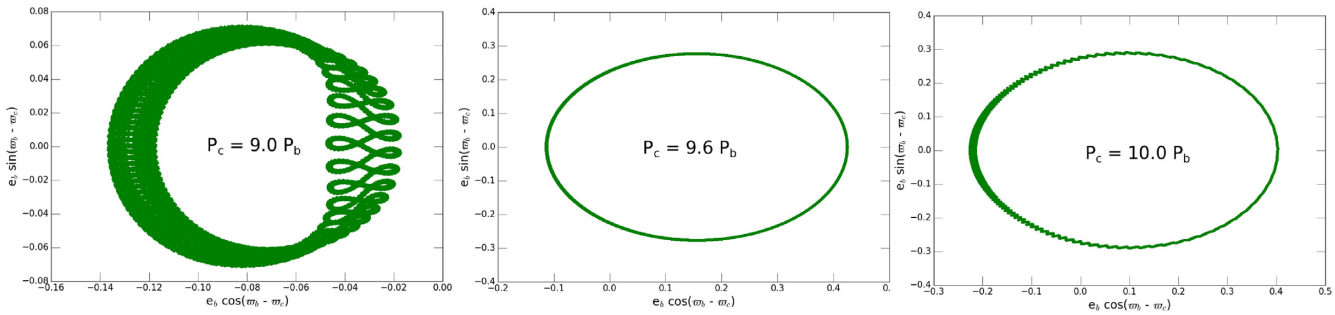

Figure 5. The evolution the system in the pseudo-coordinate-momentum phase space, over 8 $\sim \times 10^3$ yr, starting at $t = 2 \times 10^6$ yr for the 20 M_J disc case (so the disc's potential is practically null). Note the different x and y scales used.

(as of 2020 August), ∼7 per cent of all of the planet hosting stars have a mass ≥1.4 $M_\odot$. Since disc and stellar masses are strongly correlated, this can be considered as a very crude estimate for the prevalence of K419-capable discs in the population that surrounded these planet hosting stars. Moreover, in the 150 transition discs survey of van der Marel et al. (2016), a similar ∼6.6 per cent of the observed population was massive enough to account for K419. These numbers however are only reflective of the disc masses, and is certainly just a theoretical upper limit on the prevalence of K419-like systems, as only a fraction of these discs will stochastically follow this formation scenario. We emphasize that the stellar mass fraction is of the *currently observed* planet-hosting stars, and not of the overall actual stellar (or planetary) population. These numbers, in addition to the results of Section 4.3 showing that K419 could have formed from a wide range of period ratios, indicate that other apsidally anti-aligned systems could be hiding in the current confirmed planets catalogue. By searching for systems with two eccentric Jovian planets with $P_{out}/P_{in} \geq 9$ orbiting massive stars, we identify Kepler-432 and Corot-20 as prime candidates, followed by possibly Kepler-539.

Multiple simplifications were used in this work. We mainly did not take into account the feedback of the planets on to the disc. We assumed axi-symmetrical discs, and did not account for angular momentum exchange between the planets and disc (Teyssandier & Lai 2019). While the disc's viscosity can damp an embedded planet's eccentricity (Bitsch et al. 2013; Sotiriadis et al. 2017), its Lindblad torques can excite it (Goldreich & Sari 2003; Duffell & Chiang 2015; Teyssandier & Ogilvie 2016) (possibly explaining the initial AMD in the system). Recently, Teyssandier & Lai (2019) used a semi-analytic model to investigate secular dynamics of two-planet systems in non axi-symmetrical discs, accounting for the planets eccentricity damping. They showed that, while for $\alpha = 10^{-2}$ the dynamics we are considering here are suppressed, moderate eccentricity growth is possible for $\alpha = 10^{-3}$. They did not explore the case of a quasi-laminar 'dead zone' disc with $\alpha = 10^{-4}$ (Gammie 1996), a possibility consistent with recent ALMA observations (Flaherty et al. 2015, 2017). Moreover, their model and also ours did not account for planet eccentricity excitation due to the disc's torques, which likely operate for such massive planets ($m_c \simeq 7M_J$) through the 3:1 Lindblad resonance (Papaloizou, Nelson & Masset 2001; Bitsch et al. 2013). These aspects merit further investigation.

Overall, our paper shows how unique exoplanetary systems architectures can be used to trace back the properties of the disc in which the planets formed. This is parallel to some exoplanets observed in mean motion resonances (GJ 876), for which disc-driven migration captures depend on disc properties (scale height and levels of turbulence; Lee & Peale 2002; Rein 2012; Batygin & Adams 2017). Unlike the case of MMR captures however, the 'capture' into the high-eccentricity secular equilibrium of Kepler-419 depends on the integrated evolution of the disc, placing a set of complementary constraints. Future models taking into account the 3D architecture of the system (Petrovich et al. 2020) will also provide additional constrains.

ACKNOWLEDGEMENTS

We thank J.R. Touma at the American University of Beirut for interesting discussions that helped guide this project. We thank an anonymous referee for their insightful comments that helped improving this manuscript. MA-D is supported through a Trottier postdoctoral fellowship. The computations were performed on the Sunnyvale cluster at the Canadian Institute for Theoretical Astrophysics (CITA).

DATA AVAILABILITY

The data underlying this article (Rebound simulations binary archives) will be shared on reasonable request to the corresponding author.

REFERENCES

Ali-Dib M., Cumming A., Lin D. N. C., 2020, MNRAS, 494, 2440
Almenara J. M. et al., 2018, A&A, 615, A90
Andrews S. M., Wilner D. J., Espaillat C., Hughes A. M., Dullemond C. P., McClure M. K., Qi C., Brown J. M., 2011, ApJ, 732, 42
Ansdell M. et al., 2016, ApJ, 828, 46
Ansdell M., Williams J. P., Manara C. F., Miotello A., Facchini S., van der Marel N., Testi L., van Dishoeck E. F., 2017, AJ, 153, 240
Barnes R., Greenberg R., 2006, ApJ, 652, L53
Batygin K., Adams F. C., 2017, AJ, 153, 120
Bergin E. A. et al., 2013, Nature, 493, 644
Binney J., Tremaine S., 2008, Galactic Dynamics: Second Edn., Princeton University Press, Princeton, NJ USA
Bitsch B., Crida A., Libert A.-S., Lega E., 2013, A&A, 555, A124
Chatterjee S., Ford E. B., Matsumura S., Rasio F. A., 2008, ApJ, 686, 580
Crida A., Morbidelli A., Masset F., 2006, Icarus, 181, 587
Dawson R. I. et al., 2014, ApJ, 791, 89
Duffell P. C., Chiang E., 2015, ApJ, 812, 94
Flaherty K. M. et al., 2015, ApJ, 813, 99
Flaherty K. M. et al., 2017, ApJ, 843, 150
Ford E. B. et al., 2012, ApJ, 750, 113
Gammie C. F., 1996, ApJ, 457, 355
Goldreich P., Sari R., 2003, ApJ, 585, 1024
Jackson J. M., Dawson R. I., Zalesky J., 2019, AJ, 157, 166

Kanagawa K. D., Muto T., Tanaka H., Tanigawa T., Takeuchi T., Tsukagoshi T., Momose M., 2016, PASJ, 68, 43
Lee M. H., Peale S. J., 2002, ApJ, 567, 596
Lega E., Morbidelli A., Nesvorný D., 2013, MNRAS, 431, 3494
Long F . et al., 2017, ApJ, 844, 99
McClure M. K . et al., 2016, ApJ, 831, 167
Murray C. D., Dermott S. F., 2000, Solar system dynamics, Cambridge University Press, Cambridge, UK
Nagasawa M., Lin D. N. C., Ida S., 2003, ApJ, 586, 1374
Owen J. E., Clarke C. J., Ercolano B., 2012, MNRAS, 422, 1880
Papaloizou J. C. B., Nelson R. P., Masset F., 2001, A&A, 366, 263
Pascucci I. et al., 2016, ApJ, 831, 125
Petrovich C., Wu Y., Ali-Dib M., 2019, AJ, 157, 5
Petrovich C., Muñoz D. J., Kratter K. M., Malhotra R., 2020, preprint (arXiv: 2008.08587)
Pringle J. E., 1981, ARA&A, 19, 137
Rafikov R. R., Silsbee K., 2015, ApJ, 798, 69
Rein H., 2012, MNRAS, 427, L21
Rein H., Liu S.-F., 2012, A&A, 537, A128
Rein H., Spiegel D. S., 2015, MNRAS, 446, 1424
Rein H., Tamayo D., 2015, MNRAS, 452, 376
Ribas Á., Bouy H., Merín B., Duchêne G., Rebollido I., Espaillat C., Pinte C., 2016, MNRAS, 458, 1029
Sotiriadis S., Libert A.-S., Bitsch B., Crida A., 2017, A&A, 598, A70
Tamayo D., Rein H., Shi P., Hernandez D. M., 2020, MNRAS, 491, 2885
Teyssandier J., Lai D., 2019, MNRAS, 490, 4353
Teyssandier J., Ogilvie G. I., 2016, MNRAS, 458, 3221
Toliou A., Tsiganis K., Tsirvoulis G., 2019, Celest. Mech. Dyn. Astron., 132, 1
van der Marel N., Verhaar B. W., van Terwisga S., Merín B., Herczeg G., Ligterink N. F. W., van Dishoeck E. F., 2016, A&A, 592, A126
van der Marel N . et al., 2018, ApJ, 854, 177
Yu M., Evans N. J., II, Dodson-Robinson S. E., Willacy K., Turner N. J., 2017, ApJ, 841, 39

APPENDIX A:

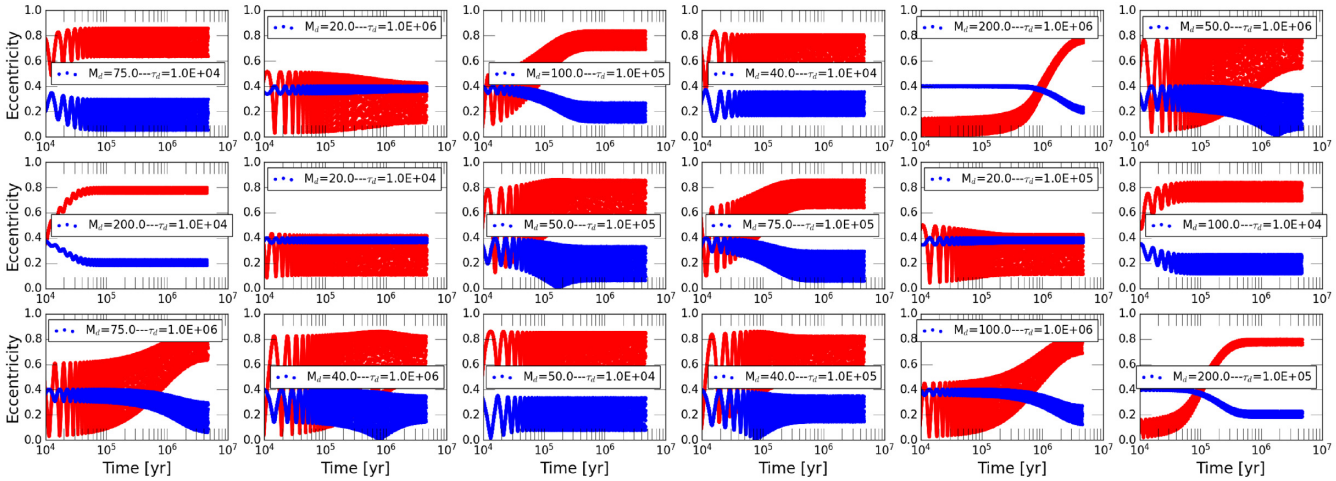

Figure A1. Kepler-419 ($P_c = 9.6\ P_b$) planets eccentricity evolution for a wide range of disc mass and dispersal time-scales. Red is for planet b, and blue is for planet c.

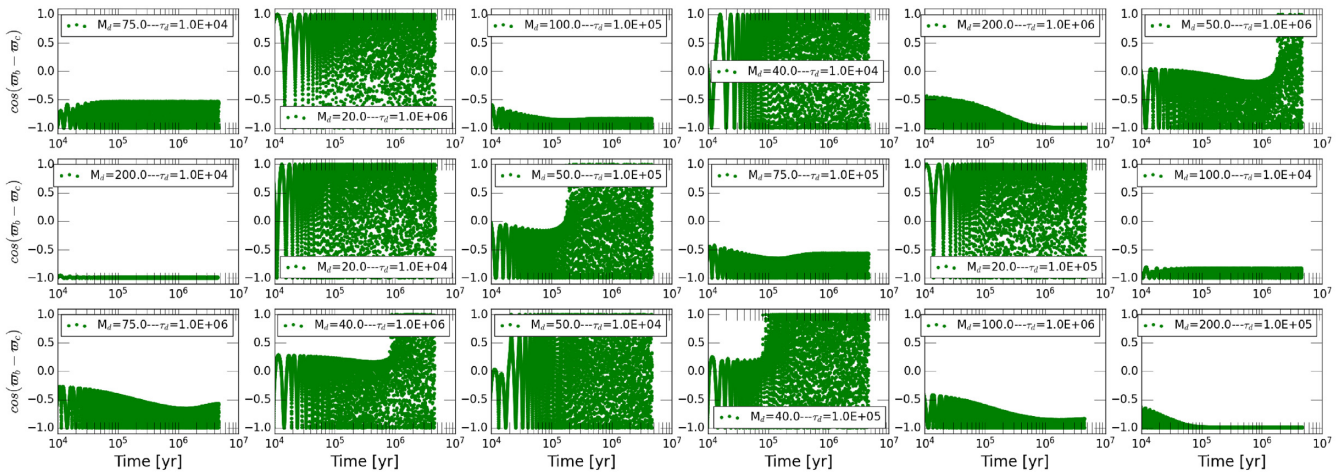

Figure A2. Kepler-419 ($P_c = 9.6\ P_b$) planets apses evolution for a wide range of disc mass and dispersal time-scales.

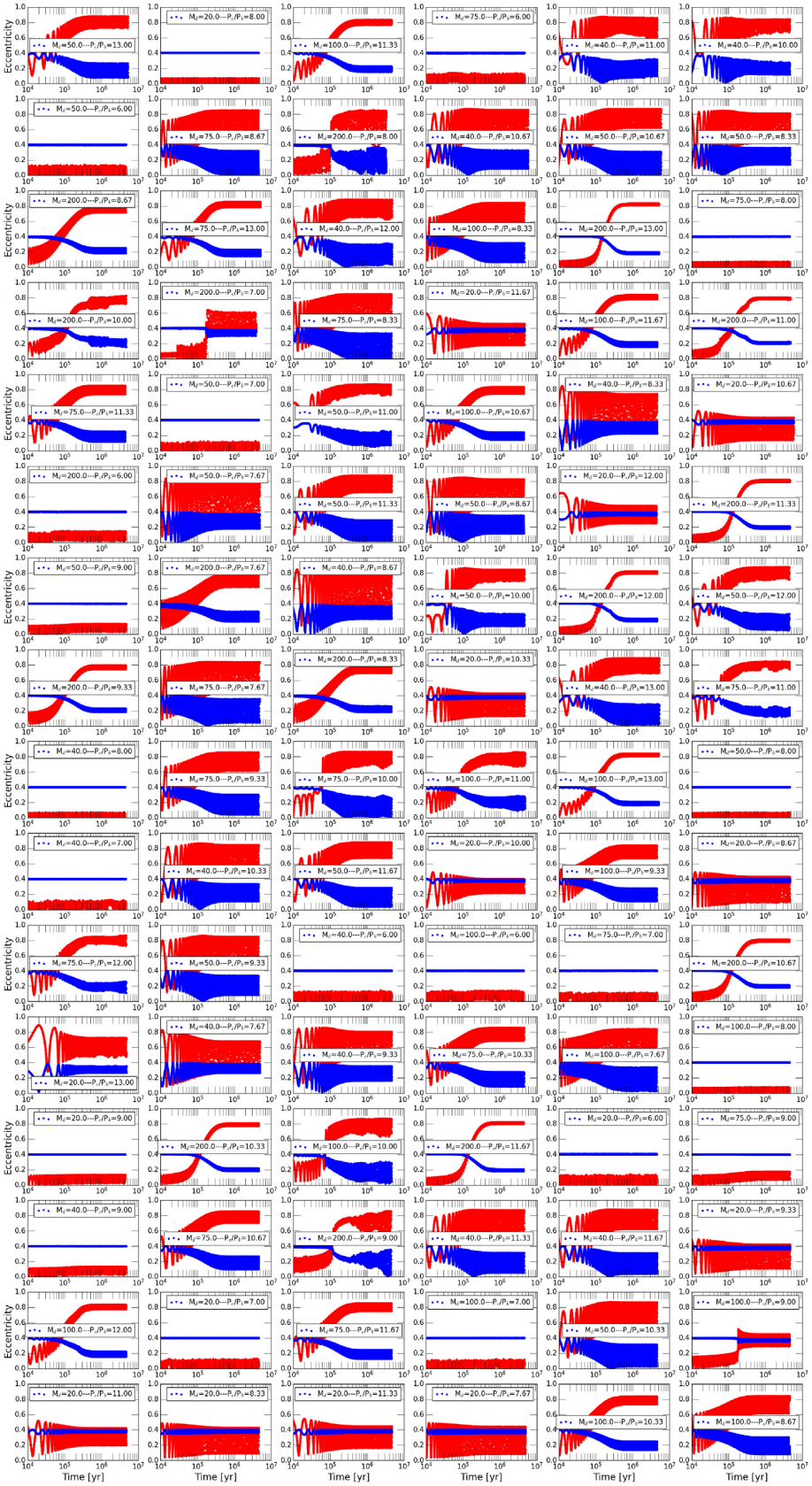

Figure A3. Same as Fig. A1, but with different semimajor axis values for planet c. Red is for planet b, and blue is for planet c.

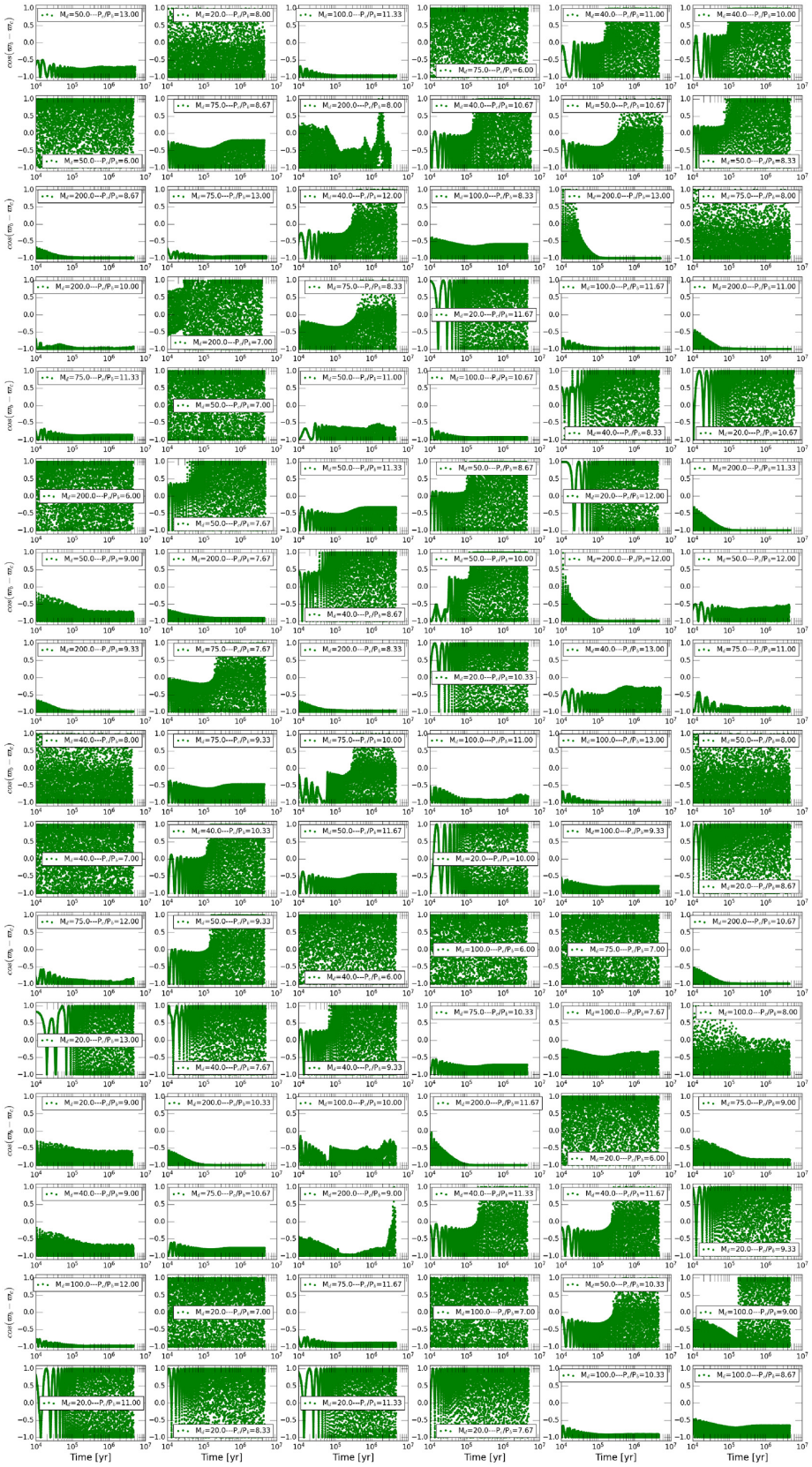

Figure A4. Same as Fig. A2, but with different semimajor axis values for planet *c*.

This paper has been typeset from a TEX/LATEX file prepared by the author.